The physical phenomena accompanying the sub-nanosecond high-voltage pulsed discharge in nitrogen

D. Levko,[1] V. F. Tarasenko,[2] and Ya. E. Krasik[1]
[1]*Department of Physics, Technion, 32000 Haifa, Israel*
[2]*Institute of High Current Electronics, 634055 Tomsk, Russia*

(Received 24 July 2012; accepted 19 September 2012; published online 15 October 2012)

Results of one-dimensional Particle-in-Cell numerical simulations of mechanism of sub-nanosecond high-voltage pulsed discharge in nitrogen are presented. It is shown that the decrease of the cathode-anode gap changes drastically both the discharge dynamics and mechanism of runaway electrons generation responsible for the discharge initiation. It is obtained that the virtual cathode exists only during tens of picoseconds for short gaps. The conditions when the virtual cathode is not formed are found. Also, the comparison between the experimental [Rybka *et al.*, Tech. Phys. Lett. **38**, 653 (2012)] and simulation results indicates the dominant role of the virtual cathode in termination of runaway electrons generation and on separate nature of emission sources from the cathode surface. [http://dx.doi.org/10.1063/1.4759048]

I. INTRODUCTION

Today high-voltage (HV) nanosecond and sub-nanosecond discharges are used for generation of high-energy electron beams which could be applied for various applications, such as x-ray generation, laser pumping, pressurized gap spark switches, etc (see, for instance, Refs. 1–3). At the present is accepted that HV nanosecond discharge in pressurized gas is initiated by the runaway electrons (RAE) generated in the vicinity of the cathode and pre-ionizing the gas inside the cathode-anode (CA) gap while propagating towards the anode. There are many theoretical,[4] numerical[3,5–11] and experimental[3,12–19] studies devoted to RAE generation during the nanosecond discharges. However, there is no generally accepted theory which can be used to describe the different experimental data obtained in experiments with cathodes having different forms, different CA gaps, gas type and pressure and different form and amplitude of the applied HV pulses. For instance, numerical research presented in Ref. 7 showed that the RAE generation during the nanosecond HV discharge is terminated by the virtual cathode (VC) formation after ≈100–300 ps of HV rise start. The VC is formed due to spatial separation between secondary electrons and ions generated in the vicinity of the cathode and when the space-charge of these secondary electrons becomes sufficient to form the potential equal to the cathode potential at that location. In addition, the absence of the pico-second time-scale resolved diagnostics does not allow comparison between the data obtained in the experiment and numerical simulations. For instance, in Ref. 16 authors used the generator SLEP-150 (140 kV output voltage with rise time of 300 ps) for generation of RAE with several tens of picoseconds duration during the rise-time of sub-nanosecond HV discharge. Also in Ref. 19 using pico-second time-resolved diagnostics, the RAE with duration of $\sim 10^{-10}$ s was described. Nevertheless, even in these experiments time resolution was ≥25 ps and thus does not allowing to obtain processes having smaller typical time duration.

In this paper, the dynamics of sub-nanosecond discharge in nitrogen will be presented with emphasizing on the role of the formation of the VC which influences significantly on the generation of RAE and HV gas discharge dynamics.

II. NUMERICAL MODEL

The processes accompanying the sub-nanosecond HV discharge in nitrogen at atmospheric pressure was studied using one-dimensional Particle-in-Cell (1D PIC) simulations applied for coaxial diode (see details in Ref. 7). A 1 cm-length cathode has radius of 3 μm and the radius of the anode was varied in the range 2–12 mm. Briefly, the sequence of 1D PIC simulation was as follows. (a) Solution of the Poisson equation at the beginning of each time step for new electron and ion space charge densities and for new boundary conditions; the anode is grounded and the cathode potential is varying in time as $\varphi_c = -\varphi_0 \sin(2\pi \cdot t/T)$, where $\varphi_0 = 140$ kV is maximal amplitude of cathode potential and $T/2 = 600$ ps is the duration of HV pulse. (b) Calculation of the number of emitted electrons defined by the field emission (FE) which is determined by the Fowler-Nordheim law.[20] (c) Solution of propagation equations for electrons and ions. (d) Electron elastic and inelastic collisions using the Monte Carlo methods, taking into account forward and backward scattering of electrons;[21] ionization and excitation of the electron levels $A^3\Sigma_u^+$ and $C^3\Pi_u$ were considered as well. (e) Particles weighting on the spatial grid and returning to step (a). The time step of $(0.5\text{-}1) \times 10^{-14}$ s allows us to consider electrons propagating only a part of the mean free path during one time step.

III. RESULTS AND DISCUSSION

At normal pressure ($P = 10^5$ Pa) in N_2 gas the value of the critical electric field E_{cr} which is necessary for electrons with the energies $\varepsilon_e > 40$ eV to become RAE is $E_{cr} \approx 4.5 \times 10^5$ V/cm.[2–4] However, FE starts at larger electric field $E_c \approx 2 \times 10^7$ V/cm, i.e., FE-electrons are emitted into CA gap when electric field in the vicinity of the cathode is significantly exceed E_{cr} and, therefore, these electrons become RAE.

It was reported in Ref. 7 that the evolution of the HV nanosecond pulsed discharge can be divided in three stages.

During the first stage, the space charge of electrons and ions is rather small and it does not change significantly the distribution of externally applied electric field. During this phase, electrons, which are emitted from the cathode and generated in the vicinity of the cathode, become RAE and pre-ionize the gas inside the entire CA gap, thus producing low-ionizes and low-conductive plasma. During the second stage of the discharge, the space charge of secondary electrons and ions becomes large enough to disturb spatial distribution of the external electric field. Also, during this stage, one obtains that at some distance from the cathode, the space separation between secondary plasma electrons and ions occurs. Results of simulations showed that the value of this distance depends on the initial conditions, i.e., gas type and pressure and rise time and amplitude of the HV pulse. The accumulation of plasma electrons leads to the formation of the VC at this location and, respectively, termination of the RAE generation from FE-electrons and electrons generated in the vicinity of the cathode. Thus, during this stage, the gas discharge develops by the RAE generated prior to the VC formation. The third stage of discharge is obtained when the electric field at the VC location from its anode side exceeds critical electric field and the VC becomes the source of RAE. However, the value of this electric field is much smaller than the electric field which one obtains at the vicinity of the cathode. Thus, the main part of these RAE has the energies smaller than 20 keV.

The results of the present simulations showed that the decrease of the CA gap d_{CA} changes significantly the dynamics of the nanosecond timescale HV gas discharge. Indeed, the time dependences of the number of RAE with $\varepsilon_e > 20$ keV and $\varepsilon_e > 1$ keV existing inside the CA gap (see Fig. 1) have different forms for different CA gaps. One can see that for RAE with $\varepsilon_e > 1$ keV RAE generation terminates (i.e., when one obtains the decrease in the number of RAE) only at $t > 0.25$ ns for $d_{CA} = 2$ mm and $d_{CA} = 4$ mm [see Fig. 1(a)] opposite to the cases with $d_{CA} \geq 6$ mm. This occurs due to the electric field at the VC location from its anode side which is $E_{VC} > E_{cr}$ right after the time t_{VC} of the VC formation. For comparison, at $t = t_{VC}$ and $d_{CA} = 12$ mm simulation shows $E_{VC} \approx 2.3 \times 10^5$ V/cm, i.e., $E_{VC} < E_{cr}$. Also, one can see [Fig. 1(b)] that the increase of the CA gap leads to decrease in the number of the RAE and in increase of the duration of RAE. The latter is caused by the later formation of the VC for larger d_{CA} and, respectively, longer duration of the RAE formed by FE-electrons and electrons from the vicinity of the cathode. The decrease of the amplitude of the number of the RAE with increase of the CA gap is related to a smaller enhancement of the electric field at the cathode by space charge of the generated ions.[7]

The value of the CA gap also determines the maximal value of the plasma density n_e, which is formed during the discharge. For instance, the results of simulations showed that $n_e \approx 5.6 \times 10^{16}$ cm^{-3} at $d_{CA} = 12$ mm, $n_e \approx 2.5 \times 10^{16}$ cm^{-3} at $d_{CA} = 8$ mm, $n_e \approx 2.8 \times 10^{16}$ cm^{-3} at $d_{CA} = 6$ mm, and $n_e \approx 8.8 \times 10^{16}$ cm^{-3} at $d_{CA} = 4$ mm. Here let us note that results of simulations showed that these values of the maximal plasma density are reached at different times of the HV pulse. The largest plasma density obtained at $d_{CA} = 4$ mm can be explained by prolonged generation of RAE with $\varepsilon_e > 1$ keV at that CA gap.

Now let us discuss two peaks in number of RAE existing in the CA gap and generated at $d_{CA} = 2$ mm and $d_{CA} = 4$ mm (see Fig. 1). The first peak in RAE generation is governed by the evolution of the VC. At this stage the RAE, which are generated from both FE-electrons and from electrons generated in the vicinity of the cathode, lose their energy by inelastic collisions and the deceleration in OK* region [see Fig. 2(a)]. When the VC is formed it generates RAE right after its formation due to $E_{VC} > E_{cr}$ at that location. However, the value of E_{VC} is smaller than the electric field in the vicinity of the cathode and, respectively, the number of electrons emitted from the VC is smaller than the number of electrons generated from FE-electrons and electrons in the vicinity of the cathode. The second stage occurs when the VC is disappeared [see Figs. 2(b) and 2(c)]. During this stage the RAE are generated from FE-electrons and electrons generated in the region A [see Fig. 2(b)] where $E > E_{cr}$. It is important to note that the second stage is not obtained for $d_{CA} > 6$ mm because at these values of the CA gap the VC is formed and exists during the entire HV rise time, as well as $E_{VC} < E_{cr}$ from its anode side.

Figs. 2(a)–2(c) shows that at $d_{CA} = 4$ mm the VC formation occurs at $t_{VC} \approx 0.112$ ns and it moves towards the anode. Nevertheless, the electric field in the vicinity of the cathode

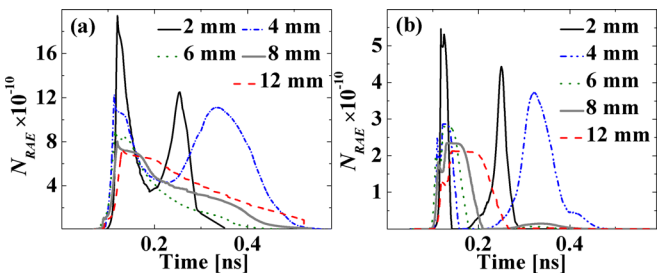

FIG. 1. Time dependence of the RAE number with $\varepsilon_e > 1$ keV (a) and with $\varepsilon_e > 20$ keV (b) at different CA gaps; $\varphi_0 = 140$ kV, $T = 1.2$ ns.

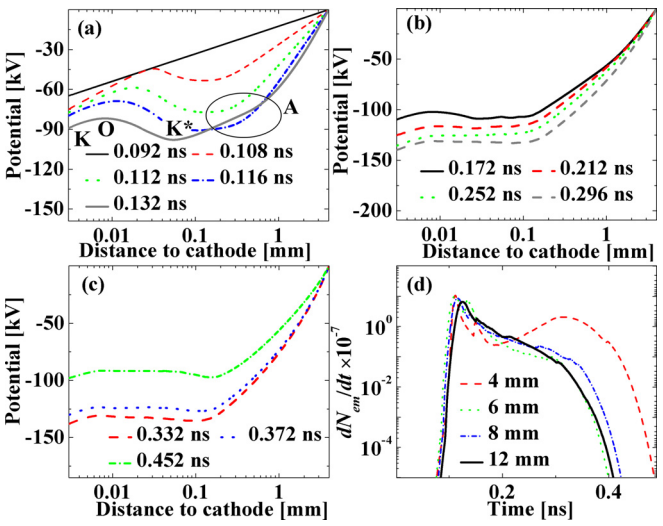

FIG. 2. (a)-(c) Potential distribution at different times for $d_{CA} = 4$ mm; (d) time dependence of the number of emitted electrons per time step dN_{em}/dt at different values of CA gap; $\varphi_0 = 140$ kV, $T = 1.2$ ns.

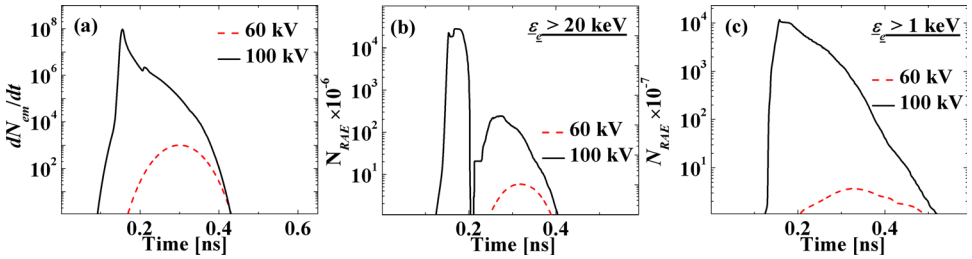

FIG. 3. (a) Time dependence of the number of electrons dN_{em}/dt emitted per each time step; time dependence of RAE with $\varepsilon_e > 20$ keV (b) and $\varepsilon_e > 1$ keV (c); $T = 1.2$ ns.

remains larger than E_{cr} and intensive FE continues [see Fig. 2(d)] with maximal duration for the case with $d_{CA} = 4$ mm. These FE-electrons experience oscillations in the potential well (KOK* region) and some of these electrons become RAE due to emission from the anode side of the VC towards the anode. Also, one can see [Figs. 2(b) and 2(c)] that the VC is disappeared at $t \approx 0.17$ ns due to neutralization by ions accelerating towards the VC in the region OK*.

Now let us consider results of simulations for smaller amplitude of the discharge voltage, namely for $\varphi_0 = 60$ kV and $\varphi_0 = 100$ kV. In the case $\varphi_0 = 60$ kV, the VC formation was not found which is explained by later and less intense FE of electrons from the cathode [see Fig. 3(a)]. This results in decrease of the rate of plasma generation and, respectively, decreases the number of RAE generated from secondary electrons in the vicinity of the cathode [see Figs. 3(b) and 3(c)]. For comparison, results of simulations showed that the largest density of the plasma at $\varphi_0 = 140$ kV is $n_e \approx 8.8 \times 10^{16}$ cm^{-3}, at $\varphi_0 = 100$ kV is $n_e \approx 2 \times 10^{16}$ cm^{-3}, and at $\varphi_0 = 60$ kV is $n_e \approx 6 \times 10^{12}$ cm^{-3}. Such large difference in the plasma density at different values of φ_0 strongly indicates the important role of FE in discharge dynamics.

As was mentioned above, the RAE pulses with duration of several tens of pico-seconds were obtained in experiments carried out by Rybka, Tarasenko *et al.* (see Ref. 13). The RAE pulses consisting of two pronounced peaks were registered in these experiments for $d_{CA} \leq 6$ mm [see Fig. 4(a)]. Moreover, it was shown that RAE related to these peaks have almost the same energies. However, the simulations carried out for similar initial conditions (HV pulse rise time, CA gap, and amplitude of cathode potential) showed that the current of RAE consists of only one peak [see Fig. 4(b)]. Also, a full width on the half maximum (FWHM) of RAE pulses obtained in experiments (~70 ps) and in simulations (~15 ps) do not agree. A short duration of the RAE beam obtained in simulations is related to fast formation of the VC which terminates generation of RAE formed from the

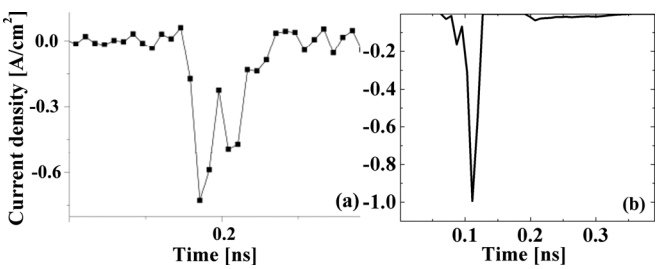

FIG. 4. Comparison between current density obtained in experiments presented in Ref. 13 (a) and in simulations (b); $d_{CA} = 6$ mm, $\varphi_0 = 140$ kV, HV rise time 300 ps.

FE-electrons and electrons generated in the vicinity of the cathode and $E_{VC} < E_{cr}$ from the VC anode side. Thus, the disagreement between experiments and simulations can be explained by the presence of two emitting centers which appearance at the cathode occurs not simultaneously but with some time delay with respect to each other. The termination of the FE of electrons from each center occurs because of the VC formation in space opposite to this center location with time delays similar to the simulation results. Formation of separate emission centers was not accounted in 1D numerical model which considered uniform FE of electrons from the entire cathode surface. Thus, results of these experiments indicated formation of VC and that the electron emission occurs from separate emission centers. Let us note that the same concern is related to the case of explosive emission centers serving as a source of RAE.

IV. CONCLUSIONS

To conclude, the results of 1D PIC simulations of sub-nanosecond HV pulsed gas discharge showed that the value of CA gap influences significantly the process of RAE generation and discharge dynamics. Namely, formation of the VC and its life-time for only tens of picoseconds at $d_{CA} < 6$ mm splits the process of the RAE generation in two stages: (a) prior and during the VC formation and (b) after the VC disappearance. Comparison between the experimental and simulation results indicates on validity of the VC formation and its dominant role in termination of RAE generation as well as on separate nature of emission sources from the cathode surface.

ACKNOWLEDGMENTS

This work was supported in part at the Technion by a fellowship from the Lady Davis Foundation.

[1]G. A. Mesyats, V. V. Osipov, and V. F. Tarasenko, *Pulsed Gas Laser* (SPIE Press, Washington, 1995).
[2]L. P. Babich, T. V. Loiko, and V. A. Tsukerman, Phys. Usp. **33**, 521 (1990).
[3]V. F. Tarasenko and S. I. Yakovlenko, Phys. Usp. **47**, 887 (2004).
[4]A. V. Gurevich and K. P. Zubin, Phys. Usp. **44**, 1119 (2001).
[5]G. A. Mesyats and M. I. Yalandin, IEEE Trans. Plasma Sci. **37**, 785 (2009).
[6]S. Ya. Belomyttsev, I. V. Romanchenko, V. V. Ryzhov, and V. A. Shklyaev, Tech. Phys. Lett. **34**, 367 (2008).
[7]D. Levko, S. Yatom, V. Vekselman, J. Z. Gleizer, V. Tz. Gurovich, and Ya. E. Krasik, J. Appl. Phys. **111**, 013303 (2012).
[8]D. Levko, S. Yatom, V. Vekselman, J. Z. Gleizer, V. Tz. Gurovich, and Ya. E. Krasik, J. Appl. Phys. **111**, 013304 (2012).
[9]D. Levko and Ya. E. Krasik, J. Appl. Phys. **111**, 013305 (2012).
[10]D. Levko, V. Tz. Gurovich, and Ya. E. Krasik, J. Appl. Phys. **111**, 013306 (2012).

[11]E. V. Oreshkin, S. A. Barengolts, S. A. Chaikovsky, and V. I. Oreshkin, Phys. Plasmas **19**, 043105 (2012).
[12]V. F. Tarasenko, E. H. Baksht, A. G.Burachenko, I. D. Kostyrya, M. I. Lomaev, and D. V. Rybka, Laser Part. Beams **26**, 605 (2008).
[13]T. Shao, Ch. Zhang, Zh. Niu, P. Yan, V. F. Tarasenko, E. Kh. Baksht, A. G. Burahenko, and Y. V. Shut'ko, Appl. Phys. Lett. **98**, 021503 (2011).
[14]H. G. Krompholz, L. L. Hatfield, A. A. Neuber, K. P. Kohl, J. E. Chaparro, and H. U. Ryu, IEEE Trans. Plasma Sci. **34**, 927 (2006).
[15]S. Yatom, V. Vekselman, J. Z. Gleizer, and Ya. E. Krasik, J. Appl. Phys. **109**, 073312 (2011).
[16]D. V. Rybka, V. F. Tarasenko, A. G. Burachenko, and E. V. Balzovskii, Tech. Phys. Lett. **38**, 657 (2012).
[17]T. Shao, Ch. Zhang, Zh. Niu, P. Yan, V. F. Tarasenko, E. Kh. Baksht, I. D. Kostyrya, and V. Shutko, J. Appl. Phys. **109**, 083306 (2011).
[18]T. Shao, V. F. Tarasenko, Ch. Zhang, M. I. Lomaev, D. A. Sorokin, P. Yan, A. V. Kozyrev, and E. Kh. Baksht, J. Appl. Phys. **111**, 023304 (2012).
[19]G. A. Mesyats, A. G. Reutova, K. A. Sharypov, V. G. Shpak, S. A. Shunailov, and M. I. Yalandin, Laser Part. Beams **29**, 425 (2011).
[20]Yu. P. Raizer, *Gas Discharge Physics* (Springer, Berlin, 1991).
[21]Y. Itikawa, J. Phys. Chem. Ref. Data **35**, 31 (2006).